Petroleum Science 20 (2023) 3223–3230

Contents lists available at ScienceDirect

Petroleum Science

journal homepage: www.keaipublishing.com/en/journals/petroleum-science

Original Paper

Preparation of a functional fracturing fluid with temperature- and salt-resistance, and low damage using a double crosslinking network

Yang Zhang [a, *], An Chen [a], Jin-Cheng Mao [a, **], Song-Hai Qin [b], Jin Li [c], Xiao-Jiang Yang [a, d], Chong Lin [a], Zhi-Yu Huang [a], Ya-Fei Liu [a]

[a] State Key Laboratory of Oil and Gas Reservoir Geology and Exploitation, Southwest Petroleum University, Chengdu, Sichuan, 610500, China
[b] Development Division, PetroChina Southwest Oil and Gas Field Company, Chengdu, Sichuan, 610066, China
[c] Downhole Services Company, CNPC Bohai Drilling Engineering Company Ltd, Renqiu, Hebei, 062550, China
[d] Sinopec Zhongyuan Oilfield Company, Puyang, Henan, 457001, China

ARTICLE INFO

Article history:
Received 7 November 2022
Received in revised form
16 January 2023
Accepted 4 April 2023
Available online 5 April 2023

Edited by Jia-Jia Fei

Keywords:
Fracturing fluid
Temperature- and salt-resistance
Particle size
Static adsorption
Low damage

ABSTRACT

Fracturing fluids (FFs) have been widely used to stimulate the tight reservoir. However, current FFs will not only lose their rheological property at high temperatures and high salt but also show an incomplete gel-breaking property. Herein, a double crosslinking network FF with pretty superiorities in rheology and low damage to the core was constructed by introducing both physical crosslinking and chemical crosslinking into the system. The construction of double crosslinking networks enhanced the rheology of this functional FF. The particle sizes of gel-breaking fluids are mainly distributed in 1.0–10,000 nm; furthermore, for every 10,000 mg/L increase in salinity, the particle size of the gel-breaking fluid is decreased by almost half. The adsorption capacity (<1.0 mg/g) gradually decreased with the increase of salinity at 20 °C. Moreover, the adsorption of gel-breaking fluids on the rock decreased first and then kept stable with temperature increasing at a salinity of ≤30,000 mg/L, however, showed the opposite trend at 40,000 mg/L. The results of rheology, particle size, static adsorption, and core damage showed that this functional FF could be an alternative for the stimulation of a tight reservoir with high temperature and recycling of produced water with high salinity.

1. Introduction

With the continuous progress of technology in the development of reservoirs, the oil and gas in unconventional reservoirs (UCRs) have been widely developed. Due to UCRs with typic characterization including complex structure, low porosity, low permeability, high pressure, high temperature, and high salinity (Wang et al., 2012), there are high requirements for performances of fracturing fluids (FFs) in the development of UCRs. Moreover, FF, as a foreign fluid, can adsorb and retain in the porous medium of rocks, decreasing the percolation channels of oil and gas, and causing a reduction in the production of oil and gas wells (Lu et al., 2017; Xu et al., 2016; You et al., 2019), which restricts the stimulation effect of tight oil and gas reservoirs. Therefore, it is urgent to develop one FF system with both temperature- and salt-resistance and low damage to stimulate the UCRs.

To endow FFs with excellent temperature- and salt-resistance performance, different methods, such as constructing multi-networks, and reinforcing with nanoparticles (Ding et al., 2022; Zhang et al., 2022), have been reported. Specifically, the multiple networks are mainly composed of collaborating and interpenetrating covalent and non-covalent systems (Zhang et al., 2022). The covalent networks impart FFs with high stability at high temperatures and salinity, while the reversible non-covalent networks can impart FFs with high self-heal properties in the pumping process with a high shear rate. Ma et al. (2019) constructed a novel FF with double networks physically linked allyl alcohol polymer (PV)/polyacrylamide (PAM). These double network supermolecular FFs were found to have a better viscosity at high temperatures compared to the conventional PAM systems. Almubarak et al. (2019) developed a dual-polymer fracturing fluid composed of a

* Corresponding author.
** Corresponding author
E-mail addresses: y.zhang@swpu.edu.cn (Y. Zhang), jcmao@swpu.edu.cn (J.-C. Mao).

https://doi.org/10.1016/j.petsci.2023.04.005

guar derivative and a PAM family. This system exhibited excellent rheological properties and a clean and controlled breaking performance with an oxidizer.

Moreover, many reported FFs usually reduced the conductivity of fracture due to their poor breaking performance in harsh environments (high salinity and high temperature). The damage of FFs to the core is mainly relative to the viscosity, particle size, insolubility of gel-breaking fluid, and its adsorption quantity on the rock (Li et al., 2022a, 2022b; Guo et al., 2018). To decrease the core damage of gel-breaking fluid, some new systems have been developed by reducing the polymer molecular weight (Weaver et al., 2002; Xiong et al., 2014), and introducing strong hydrophilic groups (Du et al., 2022; Zhang et al., 2022), etc. In this text, some functional groups were introduced into the polymer structure with a proper molecular weight. In addition, to clarify the effect of salinity on the damage of gel-breaking fluid to the rock, we systematically investigated the change of viscosity, particle size, adsorption quantity, and core damage of gel-breaking fluid at different salinities.

Herein, a functional fracturing fluid system with a double crosslinking network was developed. The FF with a double network based on 1) physical crosslinking, which is determined by multiple intermolecular forces, such as hydrogen bonding, and hydrophobic associations. 2) chemical crosslinking, which is formed between crosslinked groups and a transition metal. The double network FF showed superior rheological performance, gel-breaking property, and low core damage rate in the high salinity, which could be an alternative for the stimulation of a tight reservoir with high temperature and recycling of produced water with high salinity.

2. Experiments and methods

2.1. Materials

Copolymer (SRP-6) and crosslinker (CL-310) in this work were prepared in the lab according to the procedure reported earlier (Zhang et al., 2023). Ammonium persulfate (APS), sodium chloride (NaCl), potassium chloride (KCl), magnesium chloride ($MgCl_2$), and calcium chloride ($CaCl_2$) were all purchased from Chengdu Kelong Chemical Reagents Corporation (Chengdu, China). Deionized water (DI water) was obtained from a water purification system. Brine is composed of 2.0% KCl+5.5% NaCl+0.45% $MgCl_2$+0.55% $CaCl_2$ and originated from evaluation measurement for properties of water-based FF. Proppant was field-grade materials. All chemicals and reagents were utilized without further purification.

2.2. Strategy of the copolymer design

Studies showed that the polymer chains will curl in a harsh environment with high salt and high temperature, decreasing the hydrodynamic volume, thus, leading to poor performance of polymer solution (Zhang et al., 2022). More seriously, the polymer may be undissolved in the brine with high salinity (Yang et al., 2020). To improve the performance of polymer solution in a harsh environment, some strategies were applied, 1) the C–C bond was used as a backbone of polymer chains, due to the high bond energy (348 kJ/mol) and rigidity. 2) some strong hydrated groups were introduced into the side chain of the copolymer, such as sulfonic groups, hydroxyl groups, ethoxy groups, etc. 3) the hydrophobic chain was grafted into the polymer chains, imparting the hydrophobic association to the polymer solution. The corresponding mechanism was shown in Fig. 1. Compared to the HPAM, the functional copolymer, SRP-6, showed a superior salt- and heat-resistance, which is attributed to the multiple functional groups decreasing the negative effect of inorganic ions on the electrostatic shielding, thickness of hydration shell and double electric layer (Tan et al., 2020). Thus, the SRP-6 solution showed good stabilization in a harsh environment.

2.3. Construction of FF using double crosslinking network

To improve the stabilization of the polymer solution further, a zirconium crosslinker, CL-310 was introduced into the SRP-6 solution. In this solution, multiple intermolecular forces were introduced into the polymer solution, including hydrogen bonds, hydrophobic association, Van der Waals' force, etc., and the optimization of polymer structure by precise polymerization, which imparts the polymer solution with superior physical network structure, leading to the high performances in temperature-, salt-, shear-resistance, and low damage. Moreover, the chemical crosslinking network structure was introduced into the polymer solution, which will promote the rheological properties of the fracturing fluid in harsh environments with high temperatures and high salinity further. Due to the presentence of double network structures in the solution, the functional fracturing fluid system will show both pretty superiorities in rheology and low damage to the core, which has a bright potential to develop a tight reservoir with high temperature and high salinity.

2.4. Rheological properties

The thermal shear of different FFs was all measured on a HAAKE MARS III rheometer with a cylinder at 170 s^{-1} and different temperatures (110, 120, 150, 200 °C). The angular frequency (0.1–100 Hz) and the creep property of FF with different salinities were conducted on the Anton Paar MCR 302 rheometer with CP50-1-SN30644 plate fixture with a diameter of 0.099 mm at room temperature. Noteworthily, the salinity in this work only originates from the cations (Na^+, K^+, Ca^{2+}, Mg^{2+}) in the brine composed of 2.0% KCl+5.5% NaCl+0.45% $MgCl_2$+0.55% $CaCl_2$.

2.5. Properties of gel-breaking fluids

The distribution and particle size of gel-breaking fluids with different salinities were determined by dynamic light scattering with a wide-angle laser light scatterometer (Brookhaven, BI-200SM, Suffolk, NY, USA). The molecular weight of gel-breaking fluids with different salinities was conducted on a liquid chromatograph (Waters e2695). The static adsorption of different gel-breaking fluids on the rock powder was measured using the colorimetric method for starch cadmium iodide.

2.6. Core damages

The damage of the FF to the core was evaluated by calculating the reduction in matrix permeabilities after the gel-breaking fluids with different salinities flooded the core according to the evaluation criterion of SY/T 5107–2016. The core damage was calculated by Eq. (1).

$$\eta_d = \frac{K_1 - K_2}{K_2} \times 100\% \quad (1)$$

where η_d represents the core damage of gel-breaking fluid on the core in mg/g. K_1 and K_2 represent the permeabilities of the core before and after reservoir damage measured by the standard brine (2.0% KCl+5.5% NaCl+0.45% $MgCl_2$+0.55% $CaCl_2$), mD.

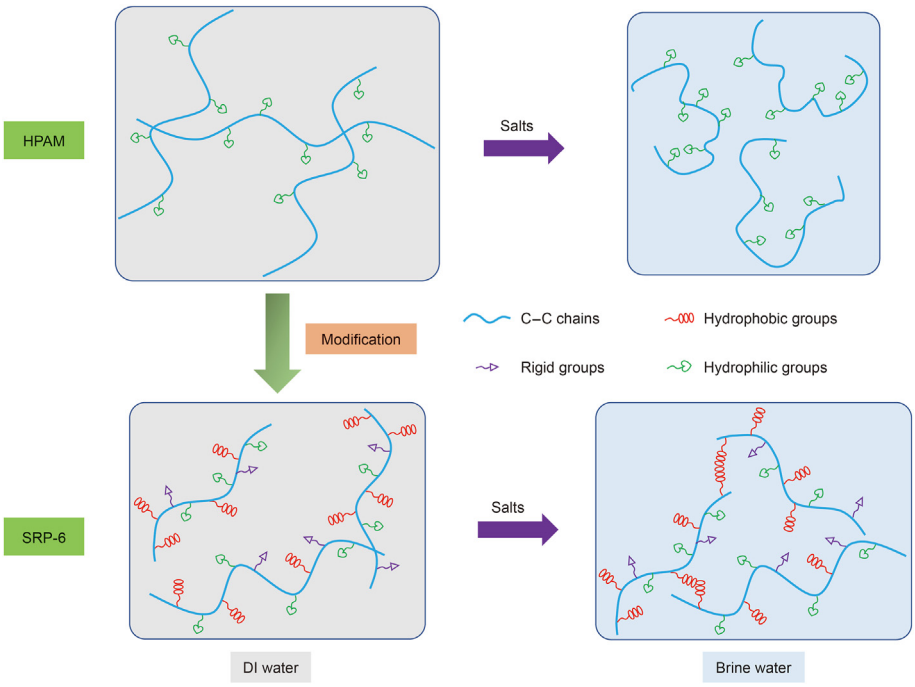

Fig. 1. The schematic diagram of the effect of salt on the HPAM and SRP-6 solution.

3. Results and discussion

3.1. Rheological property measurement

To evaluate the salt- and temperature-resistance of the functional FF, we measured the thermo-shear property of fluids with different salinities ranging from 0 to 30,000 mg/L with a step of 10,000 mg/L, at different temperatures (Fig. S1, Fig. 2(a)–(d)). Clearly, with the increase in salinity from 0 to 30,000 mg/L, the viscosities of different FFs after shearing at 170 s^{-1} for 80 min were 67.5 mPa·s (200 °C), 50.5 mPa·s (150 °C), 38 mPa·s (120 °C), and 46 mPa·s (110 °C), respectively, indicating that the maximal temperature-resistance of FFs decreased from 200 to 110 °C. At high temperatures, the metal ions will shield the electrostatic repulsion between ions on the polymer chains. In addition, the metal ions will compress the hydration film double layer, leading to the curl of polymer chains. Moreover, metal ions destroy the double electrode layer caused by the hydrogen bond between polymer molecules and water molecules (Mao et al., 2018). Thus, with the presentence of metal ions, it is inevitable to weaken the temperature resistance

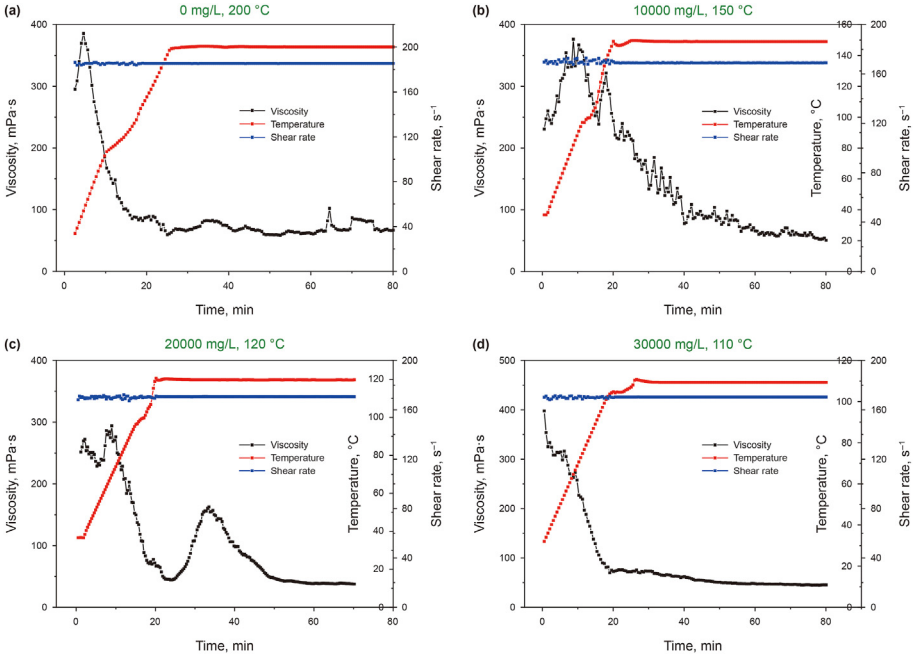

Fig. 2. The thermal shear of FF at different salinities (**a**) 0 mg/L, (**b**) 10,000 mg/L, (**c**) 20,000 mg/L, (**d**) 30,000 mg/L.

of FFs. However, the performance of FFs at different application scenarios almost all meet the requirements in industrial standards, indicating that the as-prepared FFs have great salt- and temperature-resistance.

To investigate the effect of salinity on the viscoelasticity of FFs, frequency scanning was conducted using the rheometer at 0.1 Pa and 25 °C. As shown in Fig. 3(a), with the increase in frequency, the storage modulus (G') and loss modulus (G'') all increased in the linear viscoelastic area. Moreover, with the increase in salinity, the storage moduli are all larger than the loss moduli for different fluids, interestingly, except for the fluid with a salinity of 10,000 mg/L. With the increase of salinity, the weak intermolecular forces, such as hydrogen bonds, and Van der Waals' forces, are destroyed by the metal salts, leading to a decrease in viscosity and elasticity of fluids (with a salinity of <10,000 mg/L). With the increase in salinity further, the polarity of the solution increases, promoting the formation of a hydrophobic association between the hydrophobic chains on polymer structures. The hydrophobic association strengthens the spatial network structure of the solution, thus, imparting superior viscoelasticity in the solution (with a salinity of >20,000 mg/L) (see Fig. 4).

In addition, the effect of salinity on the creep property of FFs was measured, as shown in Fig. 3(b). Similarly, with the increase of salinity, the strains of different fluids are almost higher than that of solution without salinity (0 mg/L), indicating that the salinity strengthens the density of spatial network structure, which agrees with the results of SEM (Fig. 3(c)). There is still a complete and strong microstructure in solution with different salinities, ensuring the high creep property for the solution. Particularly, when the salinity is up to 20,000 and 30,000 mg/L, strains are much larger than that of solution without salinity (0 mg/L), indicating that the salinity strengthens the density of spatial network structure.

3.2. Gel-breaking

After hydraulic fracturing, the difficulty in the flow of FFs is determined by the viscosity of fluids. The higher the viscosity is, the lower the flow-back rate is, thus, leading to high damage to the reservoir (Bian et al., 2016; Ren et al., 2019). To decrease the damage of FFs to the reservoir, APS is used to break the fluid with different concentrations in salinity.

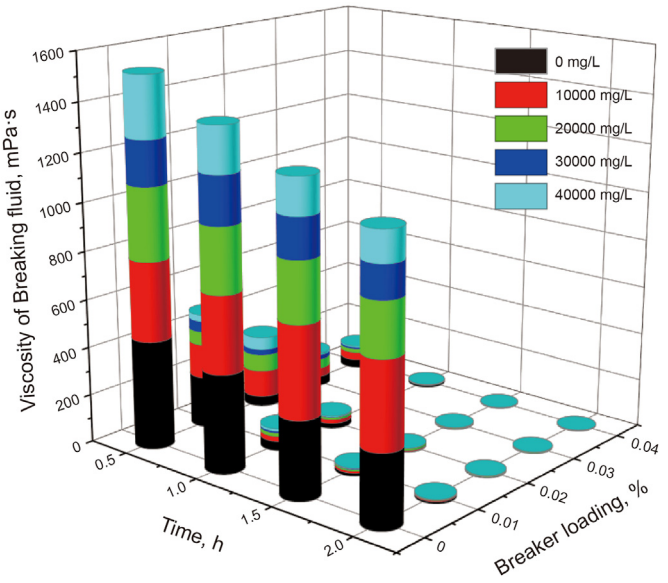

Fig. 4. The effect of salinity on the gel-breaking.

As shown in Fig. S2 and Fig. 4, with the addition of APS, fluids all are broken in 2 h completely, and no residues in fluids, indicating that FFs show a great gel-breaking property. Moreover, with the increase of salinity, time in gel-breaking decreased gradually. Specifically, when the concentration of APS is 0.04 wt%, the fluids are all broken in 1 h, except the fluid without salinity. The results are determined for three reasons: 1) the amino group and ether group on the side chain of polymer being hydrolyzed, leading to the destruction of crosslinking groups, 2) inorganic salts promoting the curly of the polymer chain, 3) due to its oxidizability, APS breaking the polymer chains. Thus, under the effect of temperature, salinity, and APS, the FFs are broken completely, ensuring the flow-back of FFs after fracking.

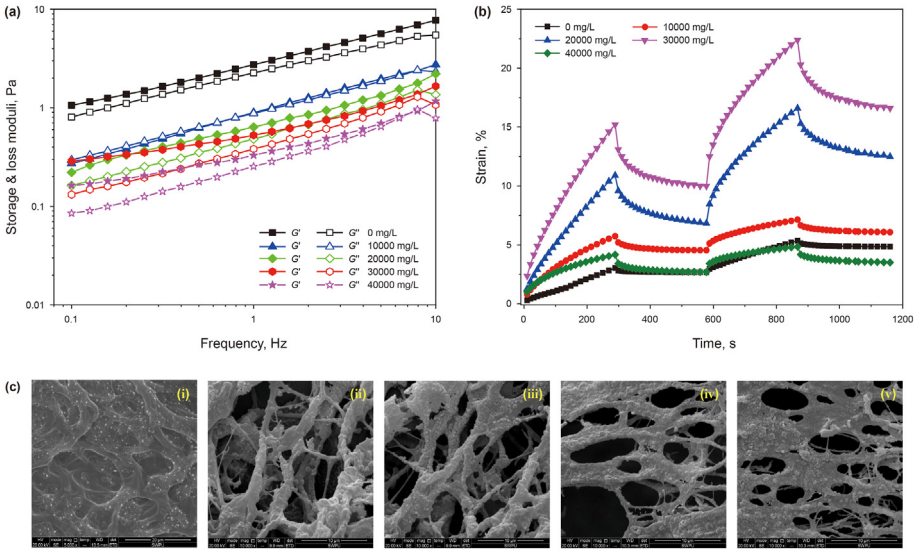

Fig. 3. (**a**) viscoelasticity and (**b**) creep property of FF at different salinities; (**c**) the network structure of FF at different salinities (i, 0 mg/L; ii, 10,000 mg/L; iii, 20,000 mg/L; iv, 30,000 mg/L; v, 40,000 mg/L).

3.3. Particle size and molecular weight of the gel-breaking fluid

As shown in Fig. S3, compared to a lot of residues in gel-breaking fluids based on hydroxypropyl guar gum (HPG), there are no visual residues in that based on SRP-6. During the gel-breaking process, the solubility of the HPG molecule decreased gradually, resulting in the formation of a floccule (Guo and He, 2012). Differently, the SRP-6 macromolecule is broken into micro-molecule with high solubility, leading to a transparent fluid. Thus, the SRP-6 solution has better-gel-breaking properties than HPG-based FFs.

To measure the damage of SRP-6-based FFs and HPG-based FFs, the distribution and particle size of gel-breaking fluids were measured when 0.03 wt% loading APS was used to break the FFs, as shown in Fig. 5 and Fig. S4. Clearly, the particle sizes of all gel-breaking fluids mainly distributed a range from 1.0 to 10,000 nm, which is attributed to the random degradation of APS to polymer chains. At the same time, the particle size of HPG-based FFs in DI water (867.2 nm) is far less than that of SRP-6-based FFs in DI water (1,632.7 nm), indicating that the HPG molecule was broken into smaller pieces than SRP-6 molecule. It is analyzed that there are a lot of ether bonds in the HPG molecule, which is sensitive to be oxidized by APS. However, as mentioned above, there are several floccules in gel-breaking fluids based on HPG. Thus, compared to SRP-6-based FFs, HPG-based FFs showed a poor gel-breaking property, which has a strong potential for formation damage.

Moreover, the particle sizes of gel-breaking fluids decreased with the increase in salinity. As shown in Fig. 5(f) and Eq. (2), for every 10,000 mg/L increase in salinity, the particle size of the gel-breaking fluid is reduced by almost half, indicating that the inorganic salt is equivalent to a “breaking promoter”, which is helpful for the break and degradation of FFs, thus, reducing the damage to the reservoir by FFs.

$$R_{n+1} = 0.5R_n + 25 \approx 0.5R_n \tag{2}$$

where R_n represents the particle size of gel-breaking fluid with a salinity of 0, 10,000, 20,000, 30,000, 40,000 in mg/L. R_{n+1} represents the particle size of gel-breaking fluid with a salinity of 10,000, 20,000, 30,000, and 40,000 in mg/L.

Except for the particle size of gel-breaking fluid, the size and distribution in molecular weight of gel-breaking fluid are also important factors affecting reservoir damage (Li et al., 2012). As shown in Fig. 6, the molecular weight of the gel-breaking fluid is all

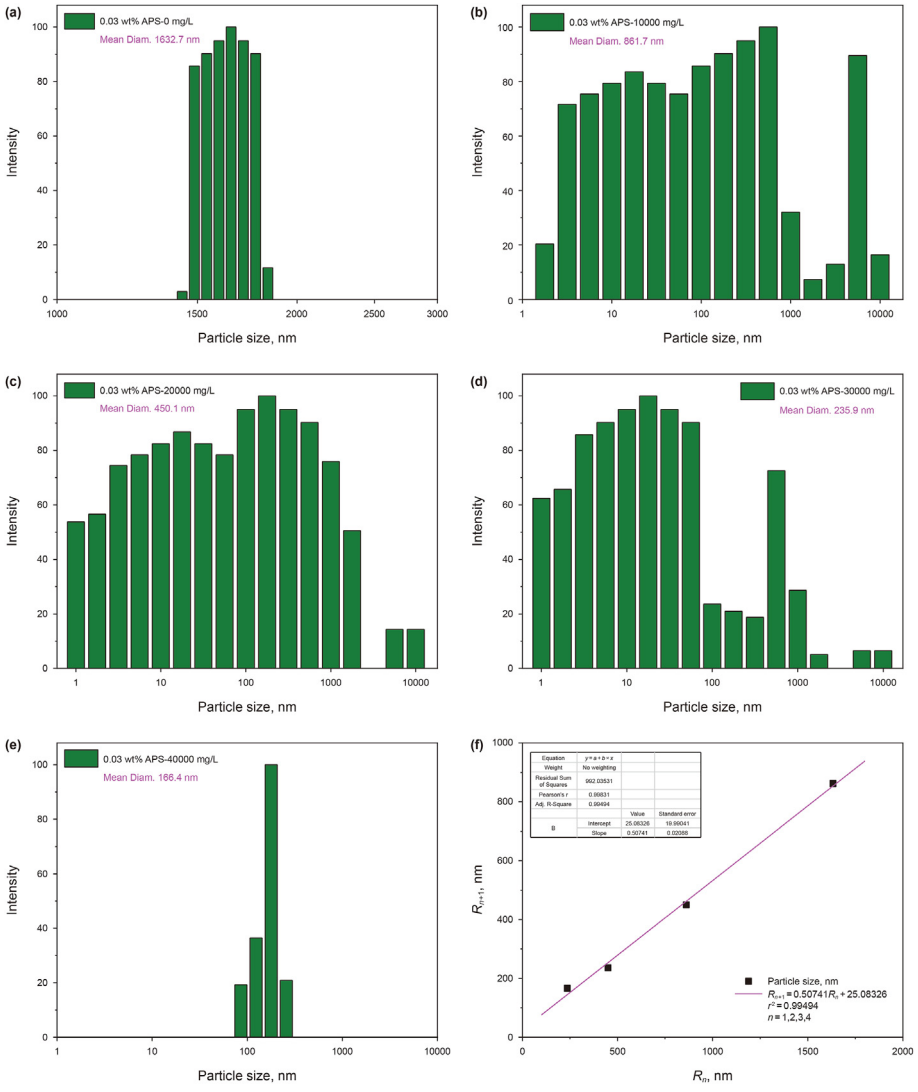

Fig. 5. The effect of salinity on the particle size of gel-breaking fluids: (**a**) 0 mg/L, (**b**) 10,000 mg/L, (**c**) 20,000 mg/L, (**d**) 30,000 mg/L, (**e**) 40,000 mg/L, (**f**) the relationship of R_n and R_{n+1}.

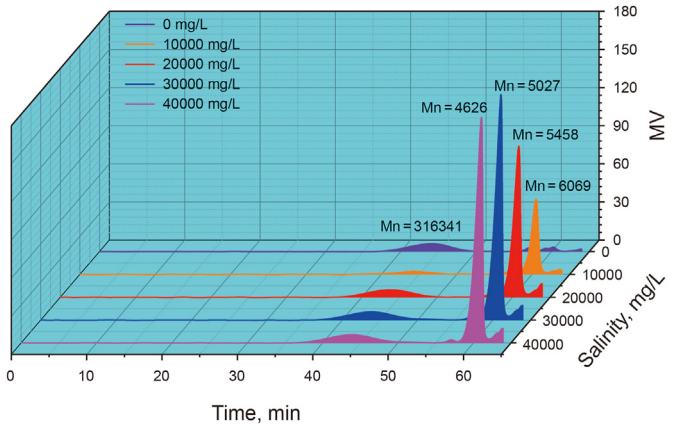

Fig. 6. The effect of salinity on the molecular weight distribution of gel-breaking fluid.

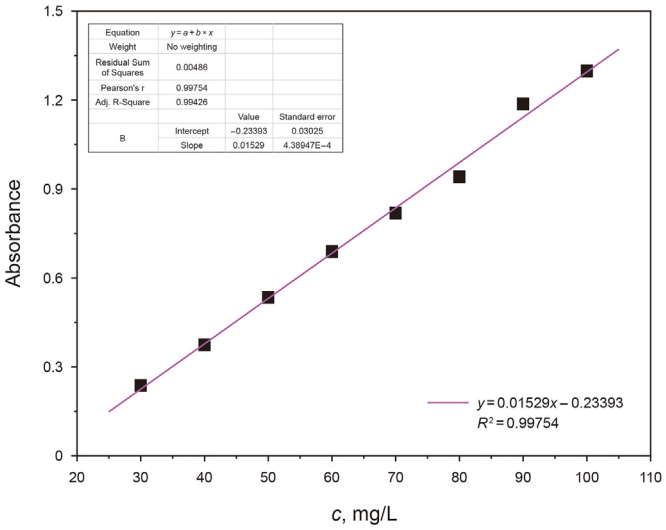

Fig. 7. Adsorption standard curve of SRP-6.

almost distributed in the range of 300,000 and 5,000 g/mol. Namely, the HPG molecule was mainly broken into two segments of different sizes during the gel-breaking process. Moreover, with the increase in salinity, the size of the molecular weight of gel-breaking fluids decreased from 6,069 g/mol (10,000 mg/L) to 4,626 g/mol (40,000 mg/L). In other words, for every 10,000 mg/L increase in salinity, the size of molecular weight of gel-breaking fluids decreased by almost 500 g/mol, indicating that the salinity promotes the gel is broken, which agrees with the results of particle size.

3.4. Static adsorption on a core of gel-breaking fluid

Studies showed that adsorption is the main damage factor to a core for polymer-based fracturing fluid (Baijal and Dey, 1982). Thus, we measured the effect of salinity on the static adsorption of gel-breaking fluid on the rock powder with a mesh of 60–100. The composition of rock powder was shown in Table S1. The starch-cadmium iodide colorimetric method was applied in this experiment (Meng et al., 2010), and the experimental principle was shown in Fig. S5.

To obtain the maximum absorption peak of copolymer SRP-6, a UV-1800 spectrophotometer was used to scan the sample from the wavelength of 200 −800 nm. The results showed that the absorption peak of copolymer SRP-6 was obtained to be maximum at the wavelength of 585 nm. Thus, the absorption of the solution with different concentrations of SRP-6 was measured at the wavelength of 585 nm. As shown in Fig. 7, the absorption at different polymer concentrations showed great linearity with a fitting degree of 0.995, indicating that the fitted curve is following Beer-Lambert law, which can be used to investigate the static adsorption of polymer on the rock powder.

According to Eq. (3), the absorption equilibrium time was investigated for a solution with a ratio of solid and liquid of 1:10 at 20 °C (Fig. 8(a)).

$$\Gamma = \frac{(c_0 - c_1) \bullet V}{W \times 1000} \tag{3}$$

where Γ represents the static adsorption of gel-breaking fluid on the surface of rock powder in mg/g. c_0 and c_1 represent initial and equilibrium concentrations of polymer in the gel-breaking fluid in mg/L. v represents the total volume of solution in the adsorption system in mL. w represents the mass of adsorbent rock powder in g.

As shown in Fig. 8(a), the adsorption of gel-breaking fluids on rock powder at different salinities all increased firstly with time and then kept stable. And all adsorption almost reached the adsorption equilibrium in 8.0 h. The whole absorption process of gel-breaking fluid on the surface of the rock is mainly divided into two stages: 1) at the beginning, the gel-breaking fluid easily contacts the active center (e.g. hydroxyl group) on the surface of rock powder by hydrogen bonding or dispersion forces; 2) when the surface of the rock was completely adsorbed by gel-breaking fluids, the polymer molecules adsorbed on the surface of rock interacting with the polymer molecules in the solution by van der Waals forces and/or hydrophobic association.

Moreover, the adsorption capacity of gel-breaking fluid gradually decreased with the increase in salinity. Noticeably, the adsorption capacity of gel-breaking fluid on the rock powder was all less than 1.0 mg/g, which is less than 20% of the adsorption of guar gum on quartz sand, as reported in the literature (Yin and Wang, 2018). Due to the negative charge of rock powder, the cationic ions are absorbed on the core easier than the anionic polymer. Thus, the cationic ions hindered the absorption of the gel-breaking fluids on the sandstone surface, resulting in a decrease in the absorption of gel-breaking fluids on the sandstone surface. In addition, as mentioned in section 3.3, the particle size of the gel-breaking fluids gradually decreases with the increase in salinity. Therefore, the polymer could be broken into smaller chain segments than that in DI water, which reduces the contact between gel-breaking fluids and the sandstone, thus, decreasing its adsorption on the sandstone.

Then, we investigated the effect of temperature on the adsorption of gel-breaking fluids on the sandstone surface (Fig. 8(b)). When the salinity is less than 30,000 mg/L, the absorption capacity of gel-breaking fluids decreased first and then kept stable with the increase of temperature. However, the absorption capacity of gel-breaking fluids with a salinity of 40,000 mg/L increased first and then kept stable with the increase in temperature. It is analyzed that the adsorption of gel-breaking fluids on sandstone includes two aspects: “positive effect” and “negative effect” (Yin and Wang, 2018; Zhang et al., 2017). On the one hand, for the positive effect, the increase in temperature promotes the thermal movement of hydrophobic chains, resulting in the decrease in the hydrophobic association, which increases the adsorption opportunities of polymers on rock powder, thus, leading to the increase of the polymer adsorption. On the other hand, for the negative effect, there are three reasons: 1) as the increase of temperature, the solubility of

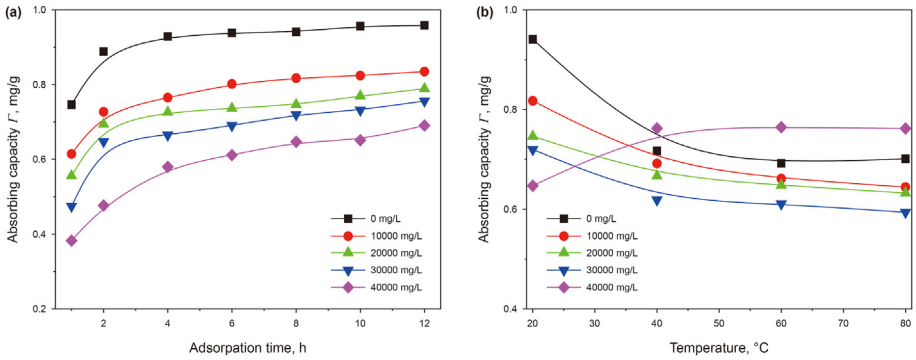

Fig. 8. The static adsorption on a core of gel-breaking fluid: (**a**) the adsorption equilibrium time of gel-breaking fluid on the lime sandstone; (**b**) the effect of temperature on the absorbing capacity of gel-breaking fluid on the lime sandstone.

the polymer in water increases, resulting in a decrease in the adsorption amount of polymer, 2) with the increase of temperature, the desorption of polymer on rock surface increases because the adsorption of polymers on rock is an exothermic process and temperature accelerates the thermal movement of polymer, 3) the interaction force between rock powder and the polymer is weakened with the increase of temperature.

As mentioned above, the effect of temperature on the adsorption is a dynamic process containing the "positive effect" and "negative effect". As shown in Fig. 8(b), with the temperature increased to 40 °C, the "positive effect" and the "negative effect" reach the same level, thus, the adsorption almost keeps stable with the increase in temperature. Moreover, with the increase of salinity, the interaction between polymers is weak, promoting the adsorption on the rock surface. As shown in Fig. 8(b), with the salinity increasing from 0 to 30,000 mg/L, the adsorption amounts decreased gradually. However, when the salinity increased to 40,000 mg/L, the adsorption amounts increased. It is analyzed that when the salinity is less than 30,000 mg/L, the negative effect caused by temperature is dominant in the solution under the consideration of temperature and salinity. When the salinity increased to 40,000 mg/L, the positive effect caused by the salinity and temperature is larger than the negative effect caused by the temperature.

3.5. Core damage

To evaluate the effect of gel-breaking fluid on the permeability of the core, the damages on the matrix permeabilities of brine with different salinities were measured with the natural cores. The results of core damage are shown in Table S2 and Fig. 9. After injecting the gel-breaking fluid into the core, the permeability all decreased. The core damage rates of gel-breaking fluids gradually decreased from 15.6% to 11.1% with the salinity increasing from 0 to 40,000 mg/L, indicating that the salinity plays a positive role in decreasing the core damage. It is investigated that adsorption is the main reason for the damage of polymers to the core (Baijal and Dey, 1982). Thus, we confirmed that the core damage rate decreased with the increase of salinity due to the adsorption decreasing with the increase of salinity.

The water contact angles (CAs) on the core slices were tested to analyze the influence of salinity on the permeability loss. Before the measurement of the CAs, the core slices were aged in ammonium chloride solution with a concentration of 3.0%, and gel-breaking fluid with different salinities for 8.0 h, respectively. Afterward, the slices were submerged in the kerosene, and DI water was dripped on the slices. The photographs of CA measurements are shown in Fig. S6. The average values of water CAs on the core slices aged in ammonium chloride solution, and gel-breaking fluid with different salinities were all far less than 90°, which is attributed to the less adsorption of gel-breaking fluid on the core. The core slice still is strong water wettability after immersing the gel-breaking fluids with different salinities, indicating that the capillary force is the driving force, which is beneficial to promote the oil and gas to flow out of the reservoir. However, the static adsorption on the core was measured by the core powder and gel-breaking fluid, and the core damage rates were obtained at room temperature in this study, which has limitations on the guidance of fracking. Thus, the dynamic adsorption and core damage at reservoir temperature will be conducted in future work, which is significant for the development of tight reservoirs.

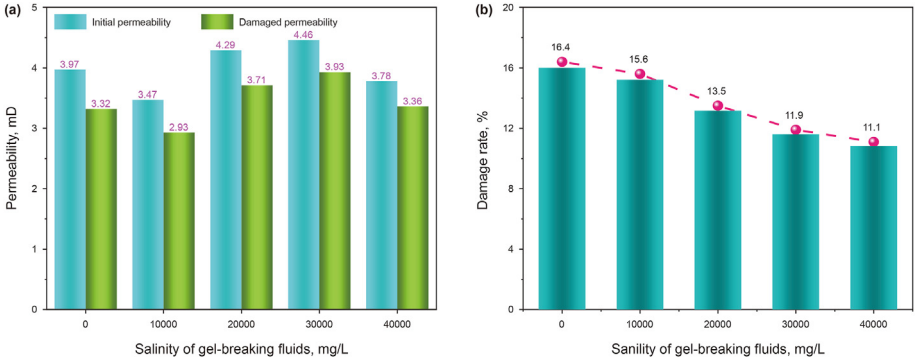

Fig. 9. Permeability damages of gel-breaking fluid with different salinities: (**a**) the permeability change and (**b**) the damage rate of the core after injecting the gel-breaking fluids.

4. Conclusions

To improve oil/gas production from the tight reservoirs with high temperatures and recycle the produced water with high salinity, a functional fracturing fluid system with pretty superiorities in rheology and low damage was constructed by optimizing the design strategy of the copolymer, and introducing the double crosslinking networks into the system. In this work, we focused on the rheological property and gel-breaking property of this functional fracturing fluid, meanwhile, some conclusions can be drawn:

(1) The functional fracturing fluid performed pretty superiorities in temperature and salt resistance, rheology (e.g., thermal shear, viscoelasticity, and creep property), and network structures with different salinities. The maximum temperature-resistance of the functional FF at 170 s^{-1} for 80 min is 200, 150, 120 and 110 °C at the salinity of 0, 10,000, 20,000, and 30,000 mg/L, respectively.
(2) The functional fracturing fluid showed the great gel-breaking property at different salinities. The particle sizes of gel-breaking fluids are mainly distributed in 1.0–10,000 nm.
(3) For every 10,000 mg/L increase in salinity, the particle size of the gel-breaking fluid is decreased by almost half and the size of the molecular weight of gel-breaking fluids decreased by almost 500 g/mol. The experimental results showed that inorganic salts are equivalent to a “breaking promoter”.
(4) The adsorption of gel-breaking fluids with different salinities on the rock powders almost reached the adsorption equilibrium in 8.0 h at 20 °C. With the increase in salinity, the adsorption capacity gradually decreased (<1.0 mg/g). The adsorption capacity of gel-breaking fluids on the rocks decreased first and then kept stable with temperature increasing at a salinity of ≤30,000 mg/L, however, showed the opposite trend at 40,000 mg/L.
(5) With the increase of salinity from 0 to 40,000 mg/L, the core damage rates gradually decreased from 16.4% to 11.1%, and the water contact angles on the core slices were all far less than 90°.
(6) Overall, with the increase of salinity, the temperature resistance of FF is weakened, and the viscosity, particle size, molecular weight, adsorption capacity, and core damage rate of gel-breaking fluid all decreased.

Declaration of competing interest

The authors declare that they have no known competing financial interests or personal relationships that could have appeared to influence the work reported in this paper.

Acknowledgments

The research is supported by the National Natural Science Foundation of China (Grant No.52274043; Grant No.52104035; Grant No.41902303), China Postdoctoral Science Foundation (2022M712646), Sichuan Innovation Team Project (2022JDTD0010), Natural Science Foundation of Sichuan Province (2023NSFSC0923), Sichuan Province Regional Innovation Cooperation Project (2020YFQ0031), and Open Fund (PLN 2021-04 and PLN 2020-13) of State Key Laboratory of Oil and Gas Reservoir Geology and Exploitation (Southwest Petroleum University).

Appendix A. Supplementary data

Supplementary data to this article can be found online at https://doi.org/10.1016/j.petsci.2023.04.005.

References

Almubarak, T., Ng, J.H., Nasr-El-Din, H.A., et al., 2019. Dual-polymer hydraulic-fracturing fluids: a synergy between polysaccharides and polyacrylamides. SPE J. 24 (6), 2635–2652. https://doi.org/10.2118/191580-PA.
Baijal, S., Dey, N., 1982. Role of molecular parameters during flow of polymer solutions in unconsolidated porous media. J. Appl. Polym. Sci. 27 (1), 121–131. https://doi.org/10.1002/app.1982.070270114.
Bian, X., Jiang, T., Wei, R., et al., 2016. Optimization of the controlling parameters of the post-frac flowback and production for normal-pressure shale-gas horizontal wells. Pet. Geol. Oilfield Dev. Daqing 35 (5), 170–174. https://doi.org/10.3969/j.issn.1000-3754.2016.05.034 (in Chinese).
Ding, Y., Gu, S., He, F., et al., 2022. Research progress on application of nanomaterials in water-based fracturing fluids. Petrochem. Technol. 51 (1), 100–106. doi:10.3969/j.issn.1000-8144.2022.01.015 (in Chinese).
Du, J., Liu, J., Zhao, L., et al., 2022. Water-soluble polymers for high-temperature resistant hydraulic fracturing: a review. J. Nat. Gas Sci. Eng. 104, 104673. https://doi.org/10.1016/j.jngse.2022.104673.
Guo, J., He, C., 2012. Microscopic mechanism of the damage caused by gelout process of fracturing fluids. Acta Pet. Sin. 33 (6), 1018–1022. https://doi.org/10.7623/syxb201206013 (in Chinese).
Guo, J., Li, Y., Wang, S., 2018. Adsorption damage and control measures of slick-water fracturing fluid in shale reservoirs. Petrol. Explor. Dev. 45 (2), 320–325. https://doi.org/10.11698/PED.2018.02.15.
Li, J., Huang, Q., Wang, G., et al., 2022a. Experimental study of effect of slickwater fracturing on coal pore structure and methane adsorption. Energy 239, 122421. https://doi.org/10.1016/j.energy.2021.122421.
Li, J., Huang, Q., Wang, G., et al., 2022b. Influence of active water on gas sorption and pore structure of coal. Fuel 310, 122400. https://doi.org/10.1016/j.fuel.2021.122400.
Li, J., Lu, H., Wang, P., et al., 2012. Research and application on enzyme breaker of fracturing in gas well. Drill. Fluid Complet. Fluid 29 (6), 71–73. https://doi.org/10.3969/j.issn.1001-5620.2012.06.022.
Lu, Y., Yang, F., Ge, Z., et al., 2017. Influence of viscoelastic surfactant fracturing fluid on permeability of coal seams. Fuel 194, 1–6. https://doi.org/10.1016/j.fuel.2016.12.078.
Ma, Y., Ma, L., Guo, J., et al., 2019. A high temperature and salt resistance supramolecular thickening system. In: Proceedings of SPE International Conference on Oilfield Chemistry. Galveston, Texas, USA. https://doi.org/10.2118/193549-MS.
Mao, J., Tan, H., Yang, B., et al., 2018. Novel hydrophobic associating polymer with good salt tolerance. Polymers 10 (8), 849. https://doi.org/10.3390/polym10080849 (in Chinese).
Meng, Z., Wei, W., Zhu, Q., et al., 2010. A study of polymer adsorption of clay minerals. Inner Mongolia Petrochemical Industry 36 (21), 14916. https://doi.org/10.3969/j.issn.1006-7981.2010.21.004 (in Chinese).
Ren, L., Di, Y., Zhao, J., et al., 2019. Advances in the theory and technique of the fracturing fluid flowback in shale gas reservoirs. Pet. Geol. Oilfield Dev. Daqing 38 (2), 144–152. https://doi.org/10.19597/j.issn.1000-3754.201803066 (in Chinese).
Tan, H., Mao, J., Zhang, W., et al., 2020. Drag reduction performance and mechanism of hydrophobic polymers in fresh water and brine. Polymers 12 (4), 955. https://doi.org/10.3390/polym12040955.
Wang, Y., Lu, Y., Li, Y., et al., 2012. Progress and application of hydraulic fracturing technology in unconventional reservoir. Acta Pet. Sin. 33 (A1), 149–158. doi:10.7623/syxb2012S1018 (in Chinese).
Weaver, J., Schmelzl, E., Jamieson, M., et al., 2002. New fluid technology allows fracturing without internal breakers. In: Proceedings of SPE Gas Technology Symposium. Canada, Calgary, Alberta. https://doi.org/10.2118/75690-MS.
Xiong, Y., Liu, Y., Shi, X., et al., 2014. Technology research of the recycled low molecular guar gum fracturing fluid. Chem. Eng. Oil Gas 43 (3), 279–283. https://doi.org/10.3969/j.issn.1007-3426.2014.03.013 (in Chinese).
Xu, L., Zhang, S., Ma, X., 2016. Characteristics of damage of guar fracturing fluid to reservoir permeability. Xinjing Pet. Geol. 37 (4), 456–459. doi:10.7657/XJPG20160413 (in Chinese).
Yang, X., Mao, J., Zhang, W., et al., 2020. Tertiary cross-linked and weighted fracturing fluid enables fracture stimulations in ultra high pressure and temperature reservoir. Fuel 268, 117222. https://doi.org/10.1016/j.fuel.2020.117222.
Yin, Z., Wang, Y., 2018. Reduced the adsorption of guar based hydraulic fracturing fluids in the formation. In: Proceedings of SPE Kingdom of Saudi Arabia Annual Technical Symposium and Exhibition. https://doi.org/10.2118/192386-MS.
You, L., Xie, B., Yang, J., et al., 2019. Mechanism of fracture damage induced by fracturing fluid flowback in shale gas reservoirs. Nat. Gas. Ind. B 6 (4), 366–373. doi:10.3787/j.issn.1000-0976.2018.12.007 (in Chinese).
Zhang, X., Zhao, F., Liu, H., 2017. Study on static adsorption of polymer. Contemp. Chem. Ind. 46 (3), 396–399. doi:10.13840/j.cnki.cn21-1457/tq.2017.03.004 (in Chinese).
Zhang, Y., Xiao, S., Mao, J., et al., 2023. Construction of a novel fracturing fluid with high viscoelasticity induced by mixed micelles. SPE J. 1–14. https://doi.org/10.2118/214670-PA.
Zhang, Y., Mao, J., Mao, J., et al., 2022. Towards sustainable oil/gas fracking by reusing its process water: a review on fundamentals, challenges, and opportunities. J. Petrol. Sci. Eng. 213, 110422. https://doi.org/10.1016/j.petrol.2022.110422.